New Series of Light-Emitting Polyquinolines Containing 9,9′-Spirobifluorene Units

Bing Huang,[†] Jun Li,[†] Zuoquan Jiang,[†] Jingui Qin,*[,†] Gui Yu,[‡] and Yunqi Liu[‡]

Department of Chemistry, Wuhan University, Wuhan 430072, China, and Institute of Chemistry Chinese Academy of Science, Beijing 100080, China

Received April 9, 2005; Revised Manuscript Received June 2, 2005

ABSTRACT: A new series of polyquinoline copolymers (**P1**−**P5**) containing 9,9′-spirobifluorene in the main chain were synthesized via Friedländer reactions. The emission colors of the polymers were readily tuned from blue to yellow by changing the conjugated counits. Excellent EL performances were obtained for **P5**, probably because the proper donor/acceptor pairs were rightly matched, and the charge transport was significantly balanced. The devices based on **P5** showed a maximum external quantum efficiency of 0.63% and a maximum photometric efficiency of 1.85 cd/A (at a brightness of 140 cd/m^2). Yellow-green EL with narrow full width at the half-maximum (fwhm < 70 nm) and the highest maximum luminance (1768 cd/m^2) among the currently reported polyquinolines was obtained for **P5**.

Introduction

Semiconducting polymers are of wide current interest for applications in electronic and optoelectronic devices including light-emitting diodes (LEDs),[1,2,6−8] thin film transistors,[3a−c] and photovoltaic cells.[3d,e] The vast majority of synthetic effort and structure−property studies in the field have to date been devoted to polymeric semiconductors having p-type (electron donor, hole transport)[1,2] properties. n-Type (electron acceptor, electron transport) polymeric semiconductors are urgently needed for developing more efficient and high-performance plastic electronic and optoelectronic devices. Molecules and polymers containing oxadiazole,[4a,b] benzothiadiazole,[4c] quinoxaline,[4d] and anthrazoline[4e,f] are some of the electron transport materials that have been explored for LED applications thus far. It has been well-known that polyquinolines (PQs) are intrinsic good n-type semiconducting polymers.[6−10,25] The polyquinolines also have outstanding thermal and oxidative stability, excellent mechanical strength, low relative permittivity, and low moisture absorption.[5−11] On the basis of their optical and electric properties, polyquinolines have been studied for their potential uses in electroluminescent devices,[6−8,15,25] electrochromic cells,[9] photovoltaic devices,[6c] chemosensors,[10] and nonlinear optics.[11] Many polyquinolines were developed since 1970s,[5] and their electroluminescent and photophysical properties have also been recently investigated.[6−8] However, these polyquinolines showed poor electroluminescent performance (maximum luminance < 300 cd/m^2)[6−8] and broad electroluminescence because the formation of aggregates and excimers in solid films even incorporating large hindrance substituents (long alkoxy or alkyl).[6−8]

It has been reported that spirobifluorene can be introduced into small compounds or polymeric chains to effectively suppress aggregate-forming tendency.[12−18] 9,9′-Spirobifluorene contains two biphenyl units connected by tetrahedral bonding carbon atom at the center, and two fluorene moieties are perpendicular to each other. This structure feature would be expected to minimize the close π-stacking in solid state. A series of spiro-annulated small molecules[12−14] and polymers[15−18] based on 9,9′-spirobifluorene have been synthesized and demonstrated to be amorphous with high thermal and morphological stability and high PL efficiency. When being applied into OLEDs, such spiro-annulated materials are effective to improve the stability, color purity, and quantum efficiency of the devices.[12−18] Chiang et al.[15] developed a series of polyquinolines containing 9,9′-spirobifluorene units, which possess high thermal stability and good solubility in common solvents. However, they just investigated PL properties of these polymers and did not further study the EL properties.

On the other hand, it is vital to properly balance the charge injection and transporting ability so as to achieve high efficiency in OLEDs.[19] There have been reports on the use of bipolar pairs of electron-withdrawing (hole transport)/electron-rich (electron transport) moieties such as oxadiazole/carbazole[20] and oxadiazole/thiophene[21] toward the achievement of "bipolar" or "p−n" luminescent polymers, which can remarkably improve the efficiency. In light of these observations, we synthesized a series of spiro-based polyquinolines with electron-withdrawing/electron-rich pairs in the chains. Because the 9,9′-spirobifluorene units served as a conjugation interrupt in these polymers, the emission colors were effectively tuned between blue and yellow by changing the conjugated length and the electronic structures of the conjugated counits in these polymers. To choose the right pair of electron-withdrawing/electron-rich moieties and tune the emission band, electron-rich groups such as carbazole, fluorene, bithiophene, and phenothiazine were introduced into the copolymers. The optical, luminescent, and electrochemical properties of these new polyquinoline copolymers were studied.

Results and Discussion

Synthesis and Characterization. The bisacetyl monomers **2**, **3**, **4**, **5**, and **6** were synthesized according to a general procedure via the Friedel−Crafts acylation with acetyl chloride in CS_2 or acetic anhydride/phosphoric acid, as shown in Scheme 1. **P1**−**P5** were

[†] Wuhan University.
[‡] Chinese Academy of Science.
* To whom correspondence should be addressed: Tel +86-27-68764117; Fax +86-27-68756757; e-mail jgqin@whu.edu.cn.

10.1021/ma050741q CCC: $30.25
Published on Web 07/06/2005

Scheme 1. Synthesis of Monomers 2–6

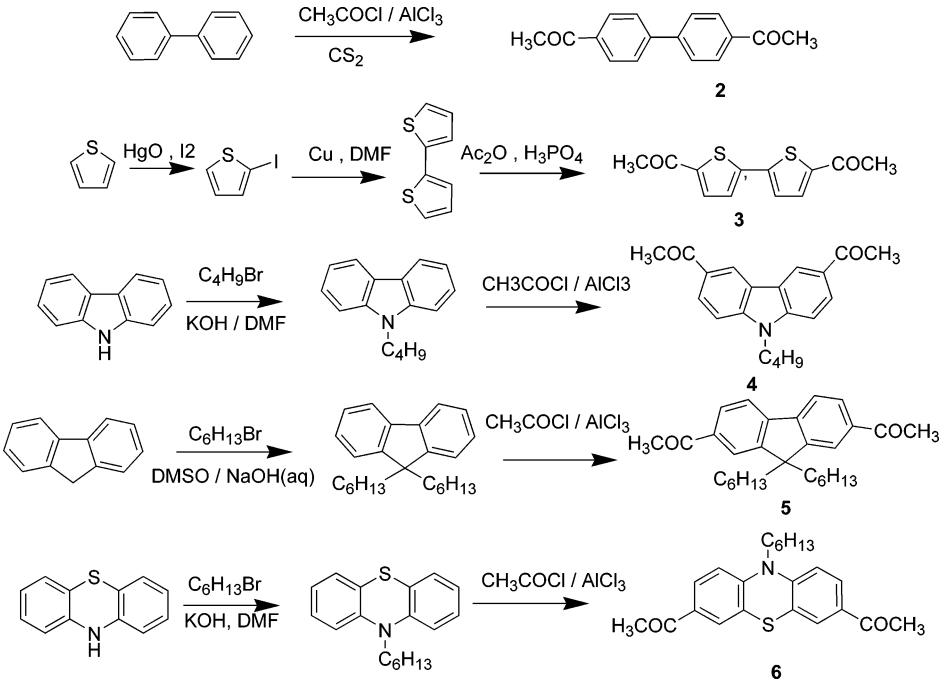

Scheme 2. Synthesis of Copolymers P1–P5

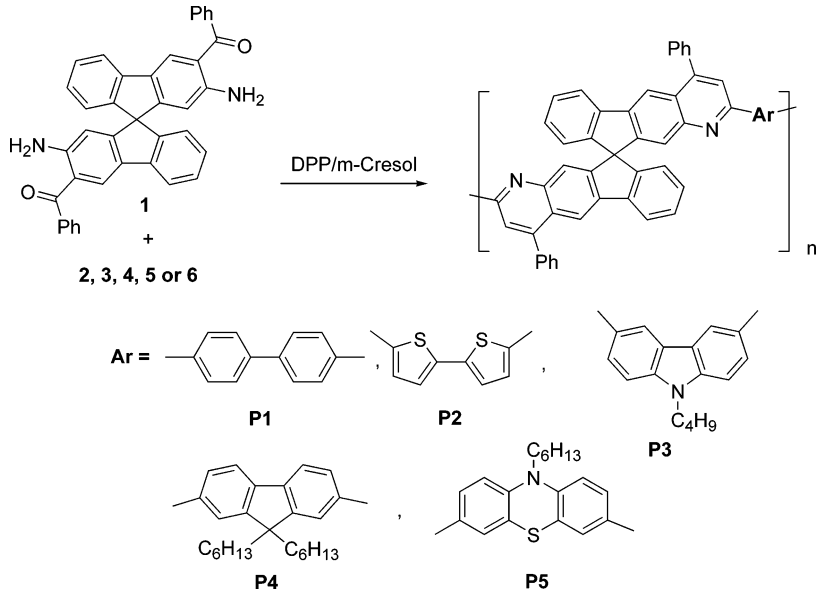

synthesized using a condensation scheme based on acid-catalyzed Friedländer[6–11,15c] reaction, as shown in Scheme 2. An equimolar mixture of the appropriate bisacetyl monomer and the bis(*o*-aminoketone) monomer **1** was reacted in an acid medium of diphenyl phosphate (DPP) and *m*-cresol at 140 °C for 72 h under argon. The resulting viscous polymer solution was diluted with $CHCl_3$ and precipitated into ethanol containing 10% triethylamine, followed by Soxhlet extraction with the same solution to obtain the polymers in good yields (56–93%). The structures of these polymers were characterized by ^{1}H NMR, ^{13}C NMR, and FT-IR spectroscopy. The proton signals from the amino and acetyl groups in the monomer structures are not observed, indicating that no significant amount of monomeric residue remained. The disappearance of characteristic doublet absorption bands of amine (3472, 3341 cm^{-1}), carbonyl stretchings of acetyl (1656–1710 cm^{-1}), and benzophenone (1628 cm^{-1}) units of the monomers and the appearance of strong bands between 1600 and 1400 cm^{-1} due to the imine (C=N) group and characteristic of the quinoline ring confirmed the complete polymerization.[6,7] The isolated polymeric materials, even those with rigid biphenyl or bithiophene linkages in the backbone, exhibited good solubility in a variety of solvents such as chloroform, tetrahydrofuran (THF), formic acid, and *m*-cresol. These results demonstrated that the introduction of a 9,9′-spirobiflorene unit into the polymer main chain was highly effective in enhancing the solubility of the polyquinolines. These copolymers were subjected to laser scattering (LS) analysis by gel permeation chromatography with THF as an eluent to yield weight-average molecular weights (M_w's) of (3.8–5.0) × 10^4. The crystallinity of the polyquinolines was evaluated by wide-angle X-ray diffraction experiments. All the polymers displayed amorphous diffraction patterns owing to the kinked 9,9′-spirobiflorene structure. The thermal properties of the copolymers were investigated through

Table 1. Molecular Weights and Thermal Properties of Polyquinolines P1−P5

polymer	M_w (×10⁴)	PD (M_w/M_n)	T_g (°C)	T_d (°C)[a]
P1	5.0	1.10	243	540
P2	4.4	1.10	259	525
P3	5.0	1.09	320	535
P4	3.8	1.07	376	420
P5	4.5	1.24	222	370

[a] Onset decomposition temperature measured by TGA under nitrogen.

Table 2. Photophysical Properties of Polyquinolines P1−P5

	solution λ_{max} (nm)		thin film λ_{max} (nm)		
polymer	abs	emis	abs	emis	φ_F[a] (sol)
P1	382	405 (428)	384	435	0.28
P2	442	(492) 520	443	542	0.38
P3	400	442	401	447 (544)	0.32
P4	388, 406	418 (442)	391	510	0.51
P5	410	546	410	550	0.16

[a] Solution quantum yields were measured relative to quinine bisulfate (in 1.0 M H_2SO_4).

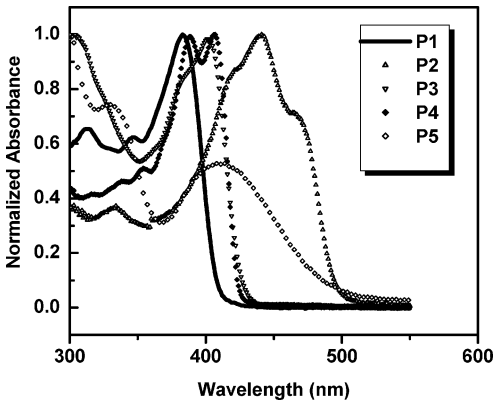

Figure 1. UV−vis absorption spectra of **P1**−**P5** in THF.

DSC and TGA, and the results are tabulated in Table 1. DSC was performed in the range from ambient temperature to 400 °C (except for **P5**, DSC was performed up to 300 °C). All the polymers have high glass transition temperatures, in the range 222−320 °C. As TGA revealed, these polymers also exhibit high decomposition temperatures of 370−540 °C. These results reflect the high thermal stability of these spiro-annulated polymers.

Optical Properties. The photophysical characteristics of **P1**−**P5** were investigated in solution and in solid state. The absorption and emission spectral data for the polymers in THF and in the films casting from solution are summarized in Table 2. The absorption spectra of the polyquinolines in diluted THF solutions and in films are illustrated in Figures 1 and 2, respectively. All the polymers show the maximum absorption in the range 382−442 nm in THF, attributed to $\pi-\pi^*$ transition. In THF, the absorption spectra of **P2**, **P3**, and **P5**, which contain a strong electron donor (bithiophene, carbazole, and phenothiazine, respectively), are red-shifted compared to the other polymers. The absorption spectra of the solutions in THF are nearly identical to the corresponding spin-coating films. Thus, the electronic transitions of the polymers are primarily determined by their molecular structures, which are insignificantly affected by their aggregation states. The optical band gaps (E_g) of the polymers are determined to be 2.36−2.98 eV from the film absorption spectra.

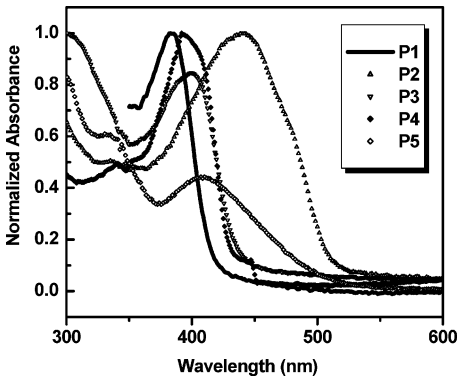

Figure 2. UV−vis absorption spectra of **P1**−**P5** in solid state.

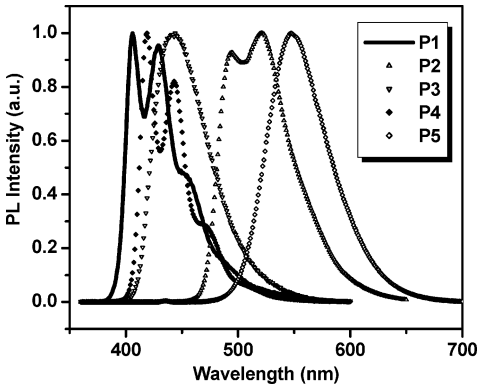

Figure 3. PL spectra of **P1**−**P5** in THF.

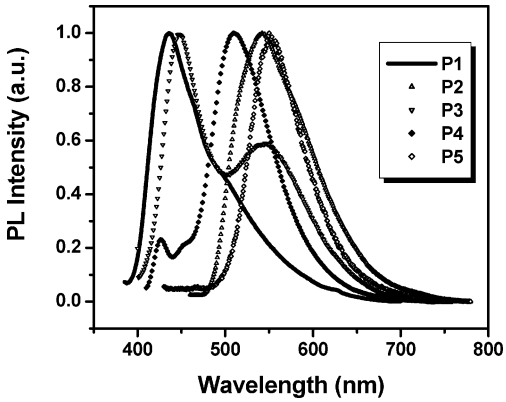

Figure 4. PL spectra of **P1**−**P5** in solid state.

Figure 3 shows the PL spectra of polymers in THF solutions. In THF, **P1** and **P4** emit strong blue fluorescence around 405−418 nm with a vibronic fine structure, **P3** emits blue fluorescence around 442 nm, **P2** emits strong green fluorescence with two peaks at 495 and 523 nm, and **P5** shows yellow-green fluorescence around 550 nm under photoexcitation. These polymers show solution PL efficiencies in THF varying from 0.16 to 0.51. For **P2**, **P3**, and **P5**, a major reason for their low emission quantum yield is their donor−acceptor nature and the consequent intramolecular charge transfer (ICT) which is known to be an important luminescence quenching mechanism in such donor−acceptor systems.[6c,e]

Figure 4 shows the PL spectra of polymers in the solid states. All the photophysical data are summarized in Table 2. Very broad emissive spectra and very large red shifts in thin films compared to solutions, which are normally observed in fully conjugated polyquinolines,[6−8] are not observed in our spiro-linked polyquinolines.

Though the solid-state PL emission spectra of the polymers showed substantial red shifts by 4−92 nm relative to dilute solutions, it is probably due to excimer formation rather than aggregation, judging by the lack of spectral shift in the absorption spectra for the solution by comparison to the solid state. The similarity of emission spectral peak maxima in PL and EL spectra further supports a lack of substantial interchain electronic interactions. As shown in Figure 4, **P1** and **P4** in solid states exhibit featureless emissions, assigned to intermolecular excimers. Thin film of the carbazole-linked polymer (**P3**) exhibits dual fluorescence, which was also observed in some carbazole-linked polyquinoline and oligomer.[6c] The blue emission band is very similar to the dilute solution emission band of **P3** in THF. On the basis of this similarity, we assign the blue emission band to singlet emission from **P3**. The featureless yellow emission band around 544 nm can be also assigned to an intermolecular excimer. A possible reason is that the spin-coated thin films of **P3** were semicrystalline, allowing highly ordered regions to coexist with amorphous regions with consequent different molecular packing and different emitting species.[6c] Surprisingly for **P5**, the solid-state emission is very similar to the dilute solution emission. Thus, the aggregates or excimers are almost completely suppressed, probably due to the steric hindrance from the long length alkyl chain of phenothiazine units and the spiro-linked structures in **P5**. The solid-state emission appears to be from an intramolecular exciton with strong charge-transfer character. The PL emission blue shift of **P2** relative to **P5**, which is the opposite of the absorption spectra relationship of the two materials, allows us to assign bithiophene-linked polymer (**P2**) emission to the dominance of intermolecular excimer. Because of insights provided by the previously discussed emission features of these copolymers, the interchain electronic interactions of the polymers are weak.

Electrochemical Properties. When materials are served as an emissive layer for OLEDs or as a donor (or acceptor) component in organic photovoltaic devices (OPVDs), matches of their valence band (HOMO) and conduction band (LUMO) energy levels with work functions of the electrodes are of paramount importance. Cyclic voltammetry is employed to investigate the redox behaviors of the polymers. Regarding the energy level of the SCE reference, one can calculate the LUMO and HOMO energies with the assumption that the energy level of SCE is 4.4 eV below vacuum.[27] In Figure 5, **P1**−**P4** show irreversible n-doping processes and irreversible (for **P1** and **P3**) or quasi-reversible (for **P2** and **P4**) oxidation processes, while **P5** exhibits a reversible reduction and oxidation process. From the onset potentials of the oxidation and reduction processes, the band gaps of the polymers are estimated to be 3.19, 2.42, 2.60, 3.18, and 2.13 eV for **P1**−**P5**, respectively. According to the empirical equations proposed by Leeuw et al.,[28] ionization potential (IP, HOMO levels) = $-([E_{onset}]^{ox} + 4.4)$ eV and electron affinities (EA, LUMO levels) = $-([E_{onset}]^{red} + 4.4)$ eV, where $[E_{onset}]^{ox}$ and $[E_{onset}]^{red}$ are the onset potentials for the oxidation and reduction of the polymer vs the reference electrode, the LUMO and HOMO energy levels are estimated. The electrochemical data of the polymers are summarized in Table 3. The electrochemical properties of **P1** and **P4** are quite similar, with large energy band gaps. As for **P2**, **P3**, and **P5**, by insertion of the electron donors (bithiophene, carbazole, and phenothiazine), decreases in the oxidation potential and energy band gap are observed, as expected initially. On the other hand, for **P2** and **P5**, obvious decrease in the oxidative onset potential and increase in the reductive onset potential are observed, which result in smaller energy gaps than **P1** and **P4**. From Table 3, we could find all the polymers have low LUMO energy levels (−2.73 to −3.03 eV). Their relatively high electron affinity and good solubility in both aprotic organic solvents (THF, chloroform, etc.) and protonic solvents (formic acid, etc.) make them very attractive for use as electron transport materials in multilayer device architectures.[6e] **P2**, **P3**, and **P5** also demonstrate hole transport properties with high HOMO energy levels from −5.07 to −5.45 eV. These data suggested **P2**, **P3**, and **P5** are characteristic of bipolar property, which could obtain excellent EL performances when serving as emissive layer in OLEDs. These results were further checked by the EL properties in the next part. Once again, the HOMO and LUMO energy levels of the polymers could be easily adjusted in the range of 0.3−1.0 eV by verifying the monomers.

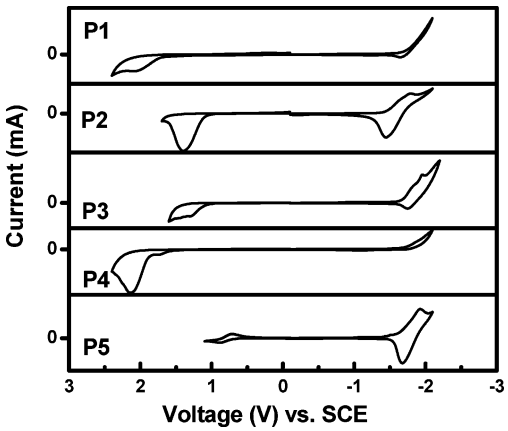

Figure 5. Cyclic voltammograms of **P1**−**P5** films coated on platinum plate electrodes in acetonitrile containing 0.1 M Bu_4NPF_6. Scan rate: 100 mV/s.

Electroluminescence. LEDs with configurations of ITO/polymer(60 nm)/Alq(30 nm)/Al(100 nm), ITO/PEDOT(50 nm)/polymer(60 nm)/Al(100 nm), or ITO/PEDOT(50 nm)/polymer(60 nm)/Alq(30 nm)/Al(100 nm) were fabricated to study the electroluminescence properties of copolymers. The device performances are summarized in Table 4. The devices based on **P4** were first investigated. Figure 7 shows the current voltage−brightness characteristic of the devices. The device of ITO/PEDOT/**P4**/Al demonstrates a blue-greenish emission as shown in Figure 6, with a maximum external quantum efficiency of 0.014% at 4 cd/m^2 and 17 V bias. The bilayer device of ITO/**P4**/Alq/Al using Alq as electron transport layer shows a decrease of turn-on voltage and an improvement of the luminance up to 302 cd/m^2, as illustrated in Figure 7, and the maximum external quantum efficiency is 6 times (0.21%) higher than that of the device of ITO/PEDOT/**P4**/Al. The EL spectra of devices based on **P4** show similar spectra around 500 nm, close to the PL spectrum in thin film, as shown in Figure 6, and shows narrow emissions (fwhm ≤ 90 nm). The aggregate formation was successfully prevented compared to the reported fluorene-linked polyquinoline,[7c] which showed broad EL emission band about 100−200 nm.

Since **P2**, **P3**, and **P5** possess electron-deficient/electron-rich moieties, they might be employed in OLED

Table 3. Electrochemical Properties of Polyquinolines P1−P5[a]

polymer	E_{red}^{o} (V)	E_{red}^{onset} (V)	LUMO (eV)[b]	E_{ox}^{peak} (V)	E_{ox}^{onset} (V)	HOMO (eV)[c]	E_g^{el} (eV)[d]	E_g^{opt} (eV)[e]
P1		−1.61	−2.79	2.08	1.58	−5.98	3.19	2.97
P2	−1.78	−1.37	−3.03	1.40	1.05	−5.45	2.42	2.40
P3	−1.96	−1.61	−2.79	1.30	0.99	−5.39	2.60	2.83
P4		−1.67	−2.73	1.75	1.51	−5.91	3.18	2.98
P5	−1.92	−1.46	−2.94	0.87	0.67	−5.07	2.13	2.36

[a] All potentials vs SCE. [b] Determined from the onset reduction potential. [c] Determined from the onset oxidation potential. [d] Electrochemical band gap estimated using $E_g^{el} = E_{ox}^{onset} - E_{red}^{onset}$. [e] Optical band gap, calculated from the absorption edge of the UV−vis spectrum.

Table 4. Performance of Single-Layer and Double-Layer LEDs Based on Polyquinolines P3−P5

device structure	V_{on}[a] (V)	B_{max}[b] (cd/m^2)	η_{max}[c] (%)	PE_{max}[d] (cd/A)	λ_{Elmax}[e] (nm)	fwhm (nm)
ITO/**P3**/Alq/Al	6	1529	0.47	1.22	509	76
ITO/PEDOT/**P4**/Al	16	57	0.014	0.028	501	90
ITO/**P4**/Alq/Al	9	302	0.085	0.21	506	82
ITO/**P5**/Alq/Al	5	1768	0.37	1.09	559	69
ITO/PEDOT/**P5**/Alq/Al	6	583	0.63	1.85	561	65

[a] Turn-on voltage, defined as the voltage needed for brightness of 1 cd/m^2. [b] Maximum brightness. [c] Maximum external quantum efficiency. [d] Maximum photometric efficiency. [e] EL emission maximum.

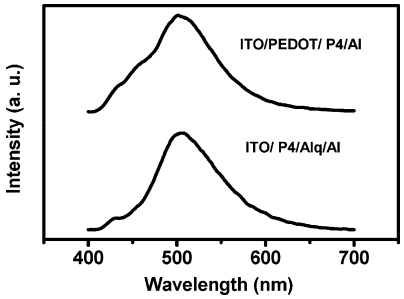

Figure 6. Normalized EL spectra of devices based on **P4**.

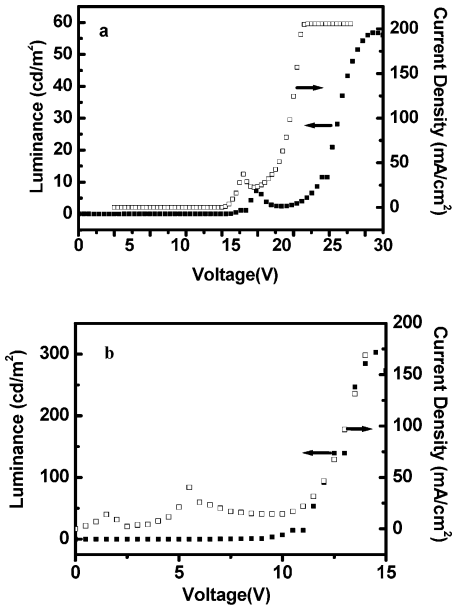

Figure 7. Current density and luminance vs applied voltage of ITO/PEDOT/**P4**/Al (a) and ITO/**P4**/Alq/Al (b).

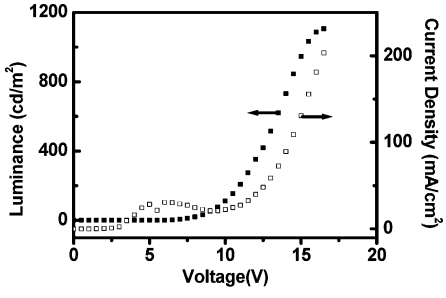

Figure 8. Current density and luminance vs applied voltage of ITO/**P3**/Alq/Al device.

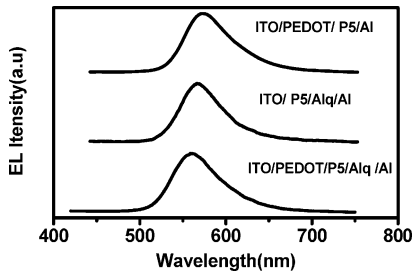

Figure 9. Normalized EL spectra of devices based on **P5**.

as electron-transporting, hole-transporting, or bifunctional materials. Initially, for **P2**, the single- or double-layer devices are hardly to observe emission due to the poor efficiency, as bithiophene is a strong donor and the effect of ICT is dominant.[6c,e] For **P3**, the single-layer device shows weak emission. A double-layer device with a configuration of ITO/**P3**/Alq/Al exhibits improved EL performance (Figure 8), and the maximum external quantum efficiency and the maximum photometric efficiency reach 0.47% and 1.22 cd/A at 487 cd/m^2 and 12 V, respectively, but Alq serves as the emitting layer and **P3** serves as the hole-transporting layer material. This observation clearly suggested that **P3** transported holes better than it carried electrons, attributed to the high HOMO energy level of **P3**. Choosing proper electron transport materials (such as TPBI or BCP) instead of Alq would help to explore the emitting properties of **P3** further. Surprising for **P5**, it is very easy to obtain a yellow emission in a device of ITO/PEDOT/**P5**/Al, as showed in Figure 9. It was reported that this kind of phenothiazine−phenylquinoline donor−acceptor polymer showed no emission in the single-layer device.[6c] To improve the device performance, two devices using Alq as electron transport material with a configuration of ITO/**P5**/Alq/Al and ITO/PEDOT/**P5**/Alq/Al were fabricated. The EL spectra of these devices (Figure 9) are similar to that of the single-layer device and PL spectrum of thin film (Figure 4), and all show very narrow emissions (fwhm < 70 nm). Figure 10 showed the current voltage−brightness characteristic of the devices. For the device of ITO/**P5**/Alq/Al, the turn-on voltage is 5 V, and the brightness reached 1768 cd/m^2

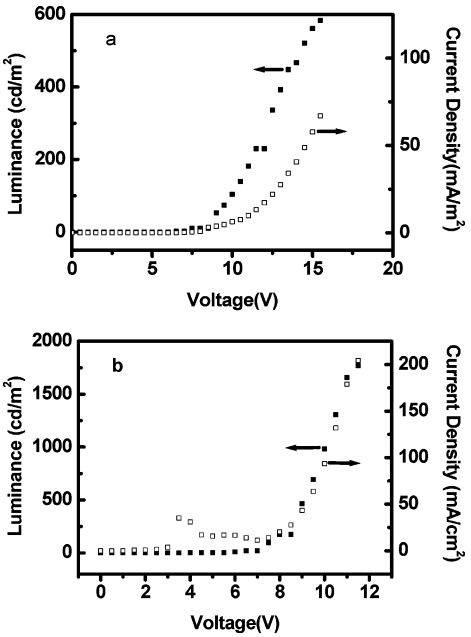

Figure 10. Current density and luminance vs applied voltage of ITO/PEDOT/**P5**/Alq/Al (a) and ITO/**P5**/Alq/Al (b).

(the highest maximum luminance among the currently reported polyquinolines) at a bias voltage of 11.5 V and a current density of 204 mA/cm^2, corresponding to an external quantum efficiency of 0.2%. The maximum external quantum efficiency is 0.37% at 694 cd/m^2 and 6 V. For the device of ITO/PEDOT/**P5**/Alq/Al, the maximum external quantum efficiency and the maximum photometric efficiency reach 0.63% and 1.85 cd/A at 140 cd/m^2 and 10.5 V, respectively. The higher efficiency than that of the device without PEDOT layer may be attributed to the good balance of charge transport and injection. Comparing **P5** to **P2** and **P3**, though the three copolymers similar possess donor/acceptor structures and demonstrated bipolar properties, only **P5** could easily obtain good EL performances, which was probably because the proper donor/acceptor pairs were chosen in **P5** and the charge transport was balanced. Considering all of the measurements were performed under ambient atmosphere at room temperature, we believed that better device performance would be possible with further optimization on device fabrication. The devices based on **P4** and **P5** all demonstrate narrow EL emissions (fwhm about 65−90 nm); thus, the introduction of spiro-units into polymeric backbones will be a promising approach to reduce the aggregates and improve the EL color purity.

Conclusions

We have described the synthesis and luminescence of a series of new polyquinoline copolymers (**P1**−**P5**) containing 9,9′-spirobifluorene in the main chain. In these copolymers, the spiro moieties not only reduced the interchain aggregates, resulting in good solubility in common organic solvents and high thermal stability, but also effectively controlled the conjugated length. The electronic and EL properties of these polymers can be readily manipulated by simply varying the nature of the counits. When the proper donor/acceptor pairs were rightly matched and the charge transport was significantly balanced (for **P5**), excellent EL performances were obtained. The devices based on **P5** showed a maximum external quantum efficiency of 0.63% and a maximum photometric efficiency of 1.85 cd/A (at a brightness of 140 cd/m^2). Yellow-green EL with narrow fwhm (<70 nm) was successfully achieved, and the highest maximum luminance (1768 cd/m^2) among the currently reported polyquinolines was obtained for **P5**. The spiro-structure modification may be a promising approach to reduce the interchain interactions and improve the color purity of polyquinolines as EL materials.

Experimental Section

Materials. The synthesis of monomer **1** was reported by Chiang and Shu in detail.[15c] Compounds **2**,[23] **3**,[24] **4**,[6c] **5**,[25] and DPP[26] (diphenyl phosphate) were prepared as described in the literature. THF was distilled from Na−K alloy, and *m*-cresol was purified by distillation under reduced pressure. CS_2 was dried over $CaCl_2$ and freshly distilled prior to use. Acetyl chloride was distilled with molecular sieve (4 A) before use. All other chemicals were used as received unless otherwise stated.

10-*n*-Hexylphenothiazine. Phenothiazine (2.0 g, 0.01 mol) was added to a suspension of potassium hydroxide (9.0 g, 0.1 mol) in 30 mL of dimethylformamide under an argon atmosphere. After 1 h of vigorous stirring, *n*-hexyl bromide (2.5 g, 0.015 mol) wad added. The reaction was carried out overnight, poured into water, and the extracted with chloroform. The extract was dried with Na_2SO_4 and then concentrated under reduced pressure. The crude product was purified by column chromatography on a silica gel column using petroleum ether as an eluent. Colorless oil was obtained (2.1 g, 74%). ^{1}H NMR (300 MHz, $CDCl_3$): δ 7.09 (d, 4 H, J = 7.5 Hz), 6.84 (dd, 4 H, J = 18, 7.5 Hz), 3.80 (t, 2 H, J = 6.6 Hz), 1.78 (t, 2 H,J = 6.6 Hz), 1.25−1.40 (m, 6 H), 0.86 (t, 3 H, J = 6.6 Hz).

2,7-Diacetyl-10-*n*-hexylphenothiazine (5). The procedure was similar to the literature[6c] with modification. To a mixture of 10-*n*-hexylphenothiazine (2.10 g, 7.4 mmol) and $AlCl_3$ (2.96 g, 22.2 mmol) in 20 mL of CS_2 in an ice−water bath was added dropwise acetyl chloride (1.7 mL, 22.2 mmol) in 5 mL of CS_2. After addition, the mixture was stirred for further 30 min and refluxed overnight. Thereafter, CS_2 was removed and the aluminum chloride complex was decomposed with a solution of crushed ice and concentrated hydrochloric acid, and then the mixture was extracted with chloroform. The organic layer was separated, washed with water, and dried over anhydrous Na_2SO_4, and the solvent was removed to dryness. The crude product was purified on silica gel column with chloroform as eluent. 0.72 g (30%) of orange solid was collected. ^{1}H NMR (300 MHz, $CDCl_3$): δ 7.73 (dd, 2 H, J = 10.2, 1.8 Hz), 7.64 (d, 2 H, J = 1.8 Hz), 6.84 (d, 2 H, J = 10.2 Hz), 3.88 (t, 2 H, J = 4.2 Hz), 2.52 (s, 6 H), 1.80 (m, 2 H), 1.25−1.44 (m, 6 H), 0.88 (t, 3 H, J = 6 Hz).

General Procedure for Polymerization. All the copolymers were synthesized according to the general literature procedures for polyquinolines.[15c] A mixture of 1 equimolar monomer **1**, 1 equimolar bisacetyl monomer, 25 equimolar diphenyl phosphate (DPP), and appropriate freshly distilled *m*-cresol was flushed with argon with stirring for about 20 min and heated from room temperature to 140 °C over about a 30 min period. It was maintained at this temperature for 72 h under an argon atmosphere. After cooling, the resulting viscous solution was diluted with chloroform and added dropwise into an agitated solution of ethanol containing 10% v/v of triethylamine. The collected polymer was purified by precipitating from chloroform into a solution of ethanol containing 10% v/v of triethylamine three times. The polymer was then continuously extracted in a Soxhlet extractor for 24 h with an ethanol solution containing 10% v/v of triethylamine and then dried at 80 °C under vacuum to give the product.

P1 (74%). ^{1}H NMR (300 MHz, $CDCl_3$): δ 6.84 (br, 2 H), 7.13 (br, 2 H), 7.35 (br, 2 H), 7.56−7.62 (br m, 16 H), 7.76 (br, 2 H), 7.86 (br, 2 H), 8.08 (br, 2 H), 8.28 (br, 2 H). ^{13}H NMR (75 MHz, $CDCl_3$): δ 68.3, 116.0, 116.8, 119.2, 121.2, 124.3, 125.0, 125.4,

126.4, 127.4, 127.9, 128.5, 129.0, 129.9, 138.5, 139.0, 140.7, 140.9, 141.3, 149.3, 149.8, 152.2, 155.6.

P2 (82%). ^{1}H NMR (300 MHz, $CDCl_3$): δ 6.80 (br, 2 H), 7.09 (br, 4 H), 7.32 (br, 2 H), 7.42 (br, 4 H), 7.58 (br m, 12 H), 7.80 (br, 2 H), 8.42 (br, 2 H). ^{13}H NMR (75 MHz, $CDCl_3$): δ 68.0, 117.2, 118.7, 12.3, 125.9, 126.1, 126.3, 127.5, 129.8, 130.1, 130.9, 139.8, 141.3, 141.6, 142.0, 145.6, 150.2, 150.8, 152.1, 153.4.

P3 (56%). ^{1}H NMR (300 MHz, $CDCl_3$): δ 0.87 (br m, 2 H), 1.27 (br m, 2 H), 1.79 (br m, 2 H), 4.22 (br, 2 H), 6.87 (br, 2 H), 7.14 (br, 2 H), 7.35 (br, 4 H), 7.61 (br m, 8 H), 7.71 (br, 4 H), 7.89 (br, 4 H), 8.24 (br, 2 H), 8.32 (br, 2 H), 8.75 (br, 2 H). ^{13}H NMR (75 MHz, $CDCl_3$): δ 14.1, 20.6, 31.3, 43.3, 65.5, 109.5, 116.1, 119.4, 119.8, 121.2, 123.7, 125.0, 125.3, 125.8, 126.0, 128.5, 128.7, 129.1, 130.0, 130.9, 139.3, 140.2, 141.3, 141.8, 142.0, 149.3, 149.5, 150.0, 152.2, 157.0.

P4 (75%). ^{1}H NMR (300 MHz, $CDCl_3$): δ 0.54−0.65 (br m, 10 H), 0.87 (br m, 12 H), 1.96 (br, 4 H), 6.82 (d, 2 H, J = 6 Hz), 7.12 (br, 2 H), 7.35 (br, 2 H), 7.59 (br, 4 H), 7.67 (br m, 10 H), 7.77 (br, 2 H), 7.87 (d, 2 H, J = 6.6 Hz), 7.96 (br, 2 H), 8.00 (d, 2 H, J = 7.2 Hz), 8.27 (br, 2 H). ^{13}H NMR (75 MHz, $CDCl_3$): δ 14.3, 22.9, 24.1, 29.9, 31.8, 40.8, 55.9, 65.5, 116.1, 119.6, 120.5, 121.2, 125.0, 125.5, 126.3, 126.7, 128.5, 128.7, 129.0, 129.9, 138.7, 139.2, 140.6, 141.0, 142.1, 149.3, 149.4, 149.9, 152.1, 156.6.

P5 (93%).^{1}H NMR (300 MHz, $CDCl_3$): δ 0.75 (br, 3 H), 1.03−1.26 (br m, 8 H), 3.76 (br, 2 H), 6.72 (br, 2 H), 6.80 (d, 2 H, J = 6 Hz), 7.09 (br, 2 H), 7.32 (br, 2 H), 7.49 (br, 2 H), 7.60 (br m, 12 H), 7.72 (br, 2 H), 7.82 (br, 2 H, J = 5.7 Hz), 8.23 (br, 2 H). ^{13}H NMR (75 MHz, $CDCl_3$): δ 14.3, 22.9, 26.7, 31.6, 46.2, 48.0, 65.4, 115.4, 116.0, 118.6, 121.1, 124.5, 124.9, 125.1, 126.1, 126.5, 128.4, 128.7, 128.9, 129.9, 133.6, 139.0, 140.3, 141.0, 145.5, 149.2, 149.8, 152.1, 154.8.

Instrumentation. ^{1}H NMR spectra were recorded on a Varian Unity 300 MHz spectrometer using $CDCl_3$ as solvent. IR spectra were obtained as KBr pellets on a Nicolet-170 SKFT-IR spectrometer. Wide-angle X-ray diffraction (WAXD) patterns were obtained at room temperature on a Shimadzu XRD 6000 powder diffractometer with Cu Kα_1 radiation (λ = 1.540 56 nm) by a graphic monochromator. Differential scanning calorimetry (DSC) was performed with a Pyris 1 DSC instrument under nitrogen at a heating rate of 15 °C/min with gas flow of 20 mL/min. Thermogravimetric analysis (TGA) was performed with a Shimadzu-DT 40 instrument at a heating rate of 20 °C/min under static argon with a gas flow of 50 mL/min. UV−vis absorption spectra were recorded on a Hitachi U-3010 UV−vis recording spectrophotometer. PL and EL spectra were performed on a Hitachi F-4500 fluorescence spectrophotometer. The molecular weights were determined by gel permeation chromatography with multiangle static light scattering (GPC-MASLS). GPC-MALLS measurements were performed on a DAWN DSP multiangle laser photometer with a pump P100 (Thermo Separation Products, San Jose, CA) equipped with a TSK-GEL G4000 HHR and a differential refractive index detector (RI-150) at 25 °C. The eluent was THF, and its flow rate was 1.00 mL/min. All solutions were filtered with sand filter and 0.45 μm filter (PTFE, Puradisc 13 mm syringe filters, Whattman, England). Astra software was utilized for data acquisition and analysis. Cyclic voltammetry (CV) were recorded on a CHI voltammetric analyzer at room temperature in CH_3CN-containing tetrabutylammonium hexafluorophosphate ($TBAPF_6$) with a scan rate of 100 mV/s. We used a platinum disk as working electrode and a silver wire as quasi-reference electrode. Ferrocene was used for potential calibration (all reported potentials are referenced against SCE).

LEDs Fabrication and Measurement. EL devices were fabricated using indium−tin oxide (ITO, 30 Ω/square) glass as an anode and aluminum (Al) as a cathode. The polymers were dissolved in chloroform and then spin-coated to ITO substrate. All the thermal evaporation was performed at about 4×10^{-4} Pa. The active area of devices was about 5 mm^2. The power of EL emission was measured using a Newport 2835-C multifunction optical meter. Current−voltage characteristics were measured with a Hewlett-Packard 4140B semiconductor parameter analyzer. All of the measurements were performed under ambient atmosphere at room temperature.

Acknowledgment. This work was supported by the National Science Foundation of China, the Scientific Research Foundation for the Overseas Chinese Scholars, State Education Ministry of China, and the National Fundamental Key Research Program of China (973 Project).

Supporting Information Available: ^{1}H and ^{13}C NMR spectra, XRD spectra, and DSC curves of polymers. This material is available free of charge via the Internet at http://pubs.acs.org.

References and Notes

(1) (a) Burroughes, J. H.; Bradley, D. D. C.; Brown, A. R.; Marks, R. N.; Mackay, K.; Friend, R. H.; Burn, P. L.; Holmes, A. B. *Nature (London)* **1990**, *347*, 539. (b) Friend, R. H.; Gymer, R. W.; Holmes, A. B.; Burroughes, J. H.; Marks, R. N.; Taliani, C.; Bradley, D. D. C.; dos Santos, D. A.; Bredas, J. L.; Logdlund, M.; Salaneck, W. R. *Nature (London)* **1999**, *397*, 121−128. (c) Ziemelis, K. *Nature (London)* **1999**, *399*, 408−411. (d) Mark, T. B.; Inbasekaran, M.; O'Brien, J.; Wu, W. *Adv. Mater.* **2000**, *12*, 1737−1750. (e) Kim, D. Y. *Prog. Polym. Sci.* **2000**, *25*, 1089−1139. (f) (g) Heeger, A. J. *Angew. Chem., Int. Ed.* **2001**, *40*, 2591−2611. (h) Barny, P. L.; Dentan, V.; Facoetti, H.; Vergnolle, M.; Vériot, G.; Servet, B.; Pribat, D. *C. R. Acad. Sci. Paris* **2000**, 493−508. (i) Cao, Y.; Parker, I. D.; Yu, G.; Zhang, C.; Heeger, A. J. *Nature (London)* **1999**, *397*, 414−417.

(2) (a) Kraft, A.; Grimsdale, A. C.; Holmes, A. B. *Angew. Chem., Int. Ed.* **1998**, *37*, 402−428. (b) Lu, J.; Tao, Y.; D'iorio, M.; Li, Y.; Ding, J.; Day, M. *Macromolecules* **2004**, *37*, 2442−2449. (c) Ego, C.; Grimsdale, A. C.; Uckert, F.; Yu, G.; Srdanov, G.; Müllen, K. *Adv. Mater.* **2002**, *14*, 809−811. (d) Yang, J.; Jiang, C.; Zhang, Y.; Yang, R.; Yang, W.; Hou, Q.; Cao, Y. *Macromolecules* **2004**, *37*, 1211−1218.

(3) (a) Ong, B. S.; Wu, Y.; Liu, P.; Gardner, S. *J. Am. Chem. Soc.* **2004**, *126*, 3378−3379. (b) Babel, A.; Jenekhe, S. A. *J. Phys. Chem. B* **2003**, *107*, 1749−1754. (c) Babel, A.; Jenekhe, S. A. *Adv. Mater.* **2002**, *14*, 371−374. (d) Brabec, C. J.; Sariciftci, N. S.; Hummelen, J. C. *Adv. Funct. Mater.* **2001**, *11*, 15−26. (e) Jenekhe, S. A.; Y, S. *Appl. Phys. Lett.* **2000**, *77*, 2635−2637.

(4) (a) Mikroyaannidis, J. A.; Spiliopoulos, I. K.; Kasimis, T. S.; Kullkarni, A. P.; Jenekhe, S. A. *Macromolecules* **2003**, *36*, 9295−9302. (b) Yang, N. C.; Lee, S. M.; Yoo, Y. M.; Kim, J. K.; Suh, D. H. *J. Polym. Sci., Part A: Polym. Chem.* **2004**, *42*, 1058−1068. (c) He, Y.; Gong, S.; Hattori, R.; Kanicki, J. *Appl. Phys. Lett.* **1999**, *74*, 2265−2267. (d) Cui, Y.; Zhang, X.; Jenekhe, S. A. *Macromolecules* **1999**, *32*, 3824−3826. (e) Tonzola, C. J.; Alam, M. M.; Kaminsky, W.; Jenekhe, S. A. *J. Am. Chem. Soc.* **2003**, *125*, 13548−13558. (f) Zhang, X.; Jenekhe, S. A. *Macromolecules* **2000**, *33*, 2069−2082.

(5) (a) Stille, J. K. *Macromolecules* **1981**, *14*, 870−880. (b) Sybert, P. D.; Beever, W. H.; Stille, J. K. *Macromolecules* **1981**, *14*, 493−502.

(6) (a) Zhang, X.; Shetty, A. S.; Jenekhe, S. A. *Macromolecules* **1999**, *32*, 7422−7429. (b) Zhang, X.; Jenekhe, S. A. *Macromolecules* **2000**, *33*, 2069−2082. (c) Jenekhe, S. A.; Lu, L.; Alam, M. M. *Macromolecules* **2001**, *34*, 7315−7324. (d) Zhang, X.; Kale, D. M.; Jenekhe, S. A. *Macromolecules* **2002**, *35*, 382−393. (e) Tonzola, C. J.; Alam, M. M.; Bean, B. A.; Jenekhe, S. A. *Macromolecules* **2004**, *37*, 3554−3563.

(7) (a) Liu, M. S.; Liu, Y.; Urian, R. C.; Ma, H.; Jen, A. K.-Y. *J. Mater. Chem.* **1999**, *9*, 2201−2204. (b) Liu, Y.; Ma, H.; Jen, A. K.-Y. *Chem. Mater.* **1999**, *11*, 27. (c) Wang, S.; Liu, Y.; Zhang, X. W.; Yu, G.; Zhu, D. B. *Synth. Met.* **2003**, *137*, 1153−1154.

(8) Krüger, H.; Janietz, S.; Sainova, D.; Wedel, A. *Macromol. Chem. Phys.* **2003**, *204*, 1607−1615.

(9) Fungo, F.; Jenekhe, S. A.; Bard, A. J. *Chem. Mater.* **2003**, *15*, 1264−1272.

(10) (a) Tong, H.; Wang, L.; Jing, X.; Wang, F. *Macromolecules* **2002**, *35*, 7169−7171. (b) Tong, H.; Wang, L.; Jing, X.; Wang, F. *Macromolecules* **2003**, *36*, 2584−2586. (c) Lee, T. S.; Yang, C.; Kim, J. L.; Lee, J.-K.; Park, W. H.; Won, Y. *J. Polym. Sci., Part A: Polym. Chem.* **2002**, *40*, 1831−1837.

(11) (a) Chen, T.-A.; Jen, A. K.-Y.; Cai, Y. M. *Chem. Mater.* **1996**, *8*, 607. (b) Jen, A. K.-Y.; Wu, X.-M.; Ma, H. *Chem. Mater.* **1998**, *10*, 471. (c) Ma, H.; Jen, A. K.-Y.; Wu, J.; Wu, X.; Liu, S.; Shu, C.-F.; Dalton, L. R.; Marder, S. R.; Thayumanavan, S. *Chem. Mater.* **1999**, *11*, 2218.
(12) (a) Wu, C.-C.; Lin, Y.-T.; Wong, K.-T.; Chen, R.-T.; Chien, Y.-Y. *Adv. Mater.* **2004**, *16*, 61−65. (b) Wu, C.-C.; Liu, T.-L.; Hung, W.-Y.; Lin, Y.-T.; Wong, K.-T.; Chen, R.-T.; Chen, Y.-M.; Chien, Y.-Y. *J. Am. Chem. Soc.* **2003**, *125*, 3710. (c) Wong, K.-T.; Chien, Y.-Y.; Chen, R.-T.; Wang, C. F.; Lin, Y.-T.; Chiang, H.-H.; Hsieh, P.-Y.; Wu, C.-C.; Chou, C. H.; Su, Y. O.; Lee, G.-H.; Peng, S. M. *J. Am. Chem. Soc.* **2002**, *124*, 11576.
(13) (a) Pudzich, R.; Salbeck, J. *Synth. Met.* **2003**, *138*, 21−31. (b) Katsis, D.; Geng, Y. H.; Ou, J. J.; Culligan, S. W.; Trajkovska, A.; Chen, S. H.; Rothberg, L. J. *Mater. Chem.* **2002**, *14*, 1332−1339. (c) Steuber, F.; Staudigel, J.; Stössel, M.; Simmerer, J.; Winnacker, A.; Spreitzer, H.; Weissörtel, F.; Salbeck, J. *Adv. Mater.* **2000**, *12*, 130−133. (d) Salbeck, J.; Yu, N.; Bauer, J.; Weissörtel, F.; Bestgen, H. *Synth. Met.* **1997**, *91*, 209−215.
(14) (a) Chen, C.-H.; Wu, F.-I.; Shu, C.-F.; Chien, C.-H.; Tao, Y.-T. *J. Chem. Mater.* **2004**, *4*, 1585−1589. (b) Lee, H.; Oh, J.; Chu, H. Y.; Lee, J.-I.; Kim, S. H.; Yang, Y. S.; Kim, G. H.; Do, L.-M.; Zyung, T.; Lee, J.; Park, Y. *Tetrahedron* **2003**, *59*, 2773−2779. (c) Geng, Y. H.; Katsis, D.; Culligan, S. W.; Ou, J. J.; Chen, S. H.; Rothberg, L. J. *Chem. Mater.* **2002**, *14*, 463−470. (d) Pei, J.; Ni, J.: Zhou, X.-H.; Cao, X.-Y.; Lai, Y.-H. *J. Org. Chem.* **2002**, *67*, 4924−4936.
(15) (a) Chen, C. H.; Shu, C.-F. *J. Polym. Sci., Part A: Polym. Chem.* **2004**, *42*, 3314−3322. (b) Wu, F. I.; Dodda, R.; Reddy, D. S.; Shu, C.-F. *J. Mater. Chem.* **2002**, *12*, 2893−2897. (c) Chiang, C.-L.; Shu, C.-F. *Chem. Mater.* **2002**, *14*, 682−687.
(16) (a) Miller, R. D.; Murphy, A. R.; Lee, V. Y.; Scott, J. C.; Bozano, L.; Smith, R.; Bacilieri, C. *Polym. Prepr.* **2002**, *43* (1), 116. (b) Marsitzky, D.; Murray, J.; Scott, J. C.; Carter, K. R. *Chem. Mater.* **2001**, *13*, 4285−4289.
(17) (a) Vak, D.; Chun, C.; Lee, C. L.; Kim, J.-J.; Kim, D.-Y. *J. Mater. Chem.* **2004**, *14*, 1342−1346. (b) Park, D. J.; Noh, Y.-Y.; Kim, J.-J.; Kim, D.-Y. *Polym. Prepr.* **2002**, *43* (1), 71.
(18) (a) Müller, C. D.; Falcon, A.; Reckefuss, N.; Rojahn, M.; Wiederhirn, V.; Rudati, P.; Frohne, H.; Nuyken, O.; Becker, H.; Meerholz, K. *Nature (London)* **2003**, *421*, 829−833. (b) Shin, D.-C.; Kim, Y.-H.; You, H.; Kwon, S.-K. *Macromolecules* **2003**, *36*, 3222−3227. (c) Yu, W.-L.; Pei, J.; Huang, W.; Heeger, A. J. *Adv. Mater.* **2000**, *12*, 828−831. (d) Kruder, W.; Spreitzer, H. US Patent 5,763,636, 1998.
(19) Li, X.-C.; Liu, Y.; Liu, M. S.; Jen, A. K.-Y. *Chem. Mater.* **1999**, *11*, 1568−1575.
(20) (a) Boyd, T. J.; Geerts, Y.; Lee, J. K.; Fogg, D. E.; Lavoie, G. G.; Sxhrock, R. R.; Rubner, M. F. *Macromolecules* **1997**, *30*, 3553−3559. (b) Peng, Z. H.; Bao, Z. N.; Galvin, M. E. *Chem. Mater.* **1998**, *10*, 2086−2090.
(21) Yu, W. L.; Meng, H.; Pei, J.; Huang, W.; Li, Y. F.; Heeger, A. J. *Macromolecules* **1998**, *31*, 4838−4844.
(22) Wu, T.-Y.; Sheu, R.-B.; Chen, Y. *Macromolecules* **2004**, *37*, 725−733.
(23) Sloan, G. J.; Vaughan, W. R. *J. Org. Chem.* **1957**, *22*, 750.
(24) Wynberg, H.; Logothetis, A. *J. Am. Chem. Soc.* **1956**, *78*, 1958−1961.
(25) Kim, J. L.; Cho, H. N.; Kim, J. K.; Hong, S. I. *Macromolecules* **1999**, *32*, 2065−2067.
(26) Brigl, P.; Müller, H. *Ber. B* **1939**, *72*, 2121−2130.
(27) (a) Agrawal, A. K.; Jenekhe, S. A. *Chem. Mater.* **1996**, *8*, 579−589. (b) Yang, C. J.; Jenekhe, S. A. *Macromolecules* **1995**, *28*, 1180−1196. (c) Alam, M. M.; Jenekhe, S. A. *J. Phys. Chem. B* **2002**, *106*, 11172−11177.
(28) De Leeuw, D. W.; Simenon, M. M. J.; Brown, A. R.; Einerhand, R. E. F. *Synth. Met.* **1997**, *87*, 53.

MA050741Q